

Co(II) and Cd(II) Complexes Based on 5-[(2-Methyl-1*H*-imidazol-1-yl)methyl]isophthalate: Syntheses, Characterization and Properties

Xiao-Chun Cheng, Xiao-Hong Zhu and Hai-Wei Kuai

Faculty of Life Science and Chemical Engineering, Huaiyin Institute of Technology, Huaian 223003, P. R. China

Reprint requests to Prof. Xiao-Chun Cheng. Fax: +86-517-83559044. E-mail: shxycheng@163.com

Z. Naturforsch. **2013**, *68b*, 1000–1006 / DOI: 10.5560/ZNB.2013-3165

Received June 10, 2013

Co(II) nitrate reacts with potassium 5-[(2-methyl-1*H*-imidazol-1-yl)methyl]isophthalate (K_2L) under hydrothermal conditions to yield a new complex $[Co(L)(H_2O)]$ (**1**). In the presence of 2-(pyridin-2-yl)-1*H*-benzo[*d*]imidazole (pybim) as auxiliary ligand, complex $[Cd(L)(pybim)]$ (**2**) can be obtained using $Cd(NO_3)_2$. Complexes **1** and **2** have been characterized by single-crystal and powder X-ray diffraction, IR, elemental and thermogravimetric analyses. Complex **1** exhibits a 2-fold interpenetrated 3D framework architecture with (10,3)-a topology; complex **2** consists of a 2D **fes** network with (4.8²) topology. The fluorescence properties of **2** were also investigated.

Key words: Cobalt(II), Cadmium(II), Structural Characterization, Fluorescence

Introduction

During the past decades, much progress in the design and synthesis of metal-organic frameworks (MOFs) has been achieved in coordination, materials and supramolecular chemistry [1–3]. Growing interest has been directed towards this field, and a great number of MOFs with fascinating structures and interesting properties were prepared and discussed as summarized in some comprehensive reviews [4–6]. Currently, the exploration of such functional crystalline materials has become the main aim of crystal engineering. It is known that functional properties of complexes are largely dependent on the nature of the metal centers and of the bridging ligands, which provide an impetus to test as many synthetic conditions as possible and to pursue structural diversity for the exploration of new multifunctional crystalline materials [7–9]. Many factors have an impact on the self-assembly process, including experimental conditions such as solvent, reaction temperature, pH, and ratio of metal-to-ligand [10–12].

Among many influential factors, the intrinsic nature of the organic ligands has been proved to play a decisive role in the formation of complexes, and *N*- and/or *O*-donor ligands are always regarded as excellent building blocks for desirable frameworks [13–16]. Recently, we have been focusing our attention on

the utilization of the new *N*- and *O*-donor ligand 5-[(2-methyl-1*H*-imidazol-1-yl)methyl]isophthalic acid (H_2L) as a building block for the construction of MOFs with variable structures. The arene-cored ligand H_2L has an advantage over other *N*- or *O*-donor ligands since it contains three coordinating groups, namely two rigid carboxylates and a flexible methylimidazole. Given the relative orientation of the two carboxylate groups and their potential variable coordination modes, such as monodentate, chelating, and bridging modes, the H_2L ligand can act as a multi-connector in the formation of complexes [17–19]. Furthermore, the flexible coordination group in H_2L has more spatial freedom to adopt different orientations, which originates from its freely axial rotation on the demand of coordinating requirements [20–22].

We report herein the syntheses and structural characterization of two new coordination polymers $[Co(L)(H_2O)]$ (**1**) and $[Cd(L)(pybim)]$ (**2**) obtained under different synthetic conditions. The fluorescence properties of complex **2** have been examined.

Results and Discussion

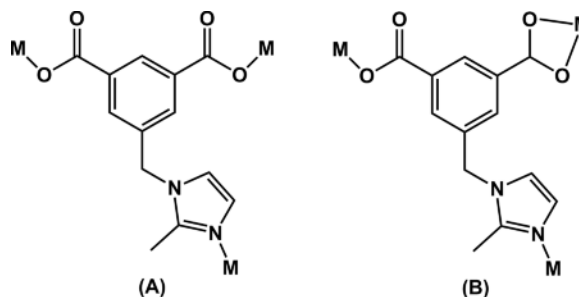
Preparation

The hydrothermal reaction of $Co(NO_3)_2 \cdot 6H_2O$ with H_2L at 180 °C leads to the formation of

complex $[\text{Co}(\text{L})(\text{H}_2\text{O})]$ (**1**); when H_2L reacts with $\text{Cd}(\text{NO}_3)_2 \cdot 4\text{H}_2\text{O}$ under the hydrothermal conditions and in the presence of pybim as an auxiliary ligand, complex $[\text{Cd}(\text{L})(\text{pybim})]$ (**2**) can be obtained. Complexes **1** and **2** are stable in air.

Structural description of $[\text{Co}(\text{L})(\text{H}_2\text{O})]$ (**1**)

X-Ray crystal structural analysis has shown that complex **1** consists of 3D frameworks crystallizing in the orthorhombic crystal system in space group $Pbca$ with $Z = 8$. The asymmetric unit of **1** contains one Co(II) atom, one L^{2-} ligand, and one coordinated water molecule (Fig. 1a). Each Co(II) cation is tetrahedrally coordinated by one methylimidazolyl nitrogen atom, two carboxylate oxygen atoms from two different L^{2-} ligands, and one oxygen atom from the coordinated water molecule. The bond lengths around Co(II) are in the range from 1.9467(15) to 2.0204(16) Å, and the bond angles are in the range of 96.03(7) to 123.79(8)° (Table 1). Both carboxylate groups adopt a $\mu_1\text{-}\eta^1\text{:}\eta^0$ -monodentate coordination mode (A in Scheme 1). Thus each L^{2-} ligand bridges three different Co(II) atoms, and each Co(II) is also coordinated by three different L^{2-} ligands. This kind of interconnection repeats infinitely to construct a neutral 3D architecture (Fig. 1b), where a layer structure can be



Scheme 1. Coordination modes of L^{2-} appearing in the complexes: A in **1**; B in **2**.

identified with the uncoordinated carboxylate groups pointing towards each side of the layer (Fig. 1c). Since both the L^{2-} ligands and the metal atoms act as 3-connected nodes, this 3D framework can be simplified as a uninodal 3-connected chiral (10, 3)-a framework (Fig. 1d) [23]. Interestingly, in the architecture of **1** there exist two self-interpenetrating networks, which are of the opposite hands and form an enantiomeric pair (Fig. 1e).

Structural description of $[\text{Cd}(\text{L})(\text{pybim})]$ (**2**)

Complex **2** crystallizes in the monoclinic system in space group $P2_1/c$ with $Z = 4$, exhibiting a 2D net-

$[\text{Co}(\text{L})(\text{H}_2\text{O})]$ (1)			
Co(1)–O(3)	1.9467(16)	Co(1)–O(5)	2.0202(16)
Co(1)–O(1)#1	1.9899(15)	Co(1)–N(11)#2	1.9986(19)
O(3)–Co(1)–O(5)	108.41(7)	O(1)#1–Co(1)–O(3)	96.03(7)
O(3)–Co(1)–N(11)#2	123.79(7)	O(1)#1–Co(1)–O(5)	106.64(7)
O(5)–Co(1)–N(11)#2	99.52(7)	O(1)#1–Co(1)–N(11)#2	121.45(7)
$[\text{Cd}(\text{L})(\text{pybim})]$ (2)			
Cd(1)–O(1)	2.340(4)	Cd(1)–O(2)	2.475(5)
Cd(1)–N(1)	2.276(6)	Cd(1)–N(2)	2.227(5)
Cd(1)–N(11)#1	2.250(5)	Cd(1)–O(4)#2	2.285(5)
O(1)–Cd(1)–O(2)	53.96(17)	O(1)–Cd(1)–N(1)	146.0(2)
O(1)–Cd(1)–N(2)	85.56(18)	O(1)–Cd(1)–N(11)#1	104.78(15)
O(1)–Cd(1)–O(4)#2	78.80(17)	O(2)–Cd(1)–N(1)	95.1(2)
O(2)–Cd(1)–N(2)	78.6(2)	O(2)–Cd(1)–N(11)#1	106.24(16)
O(2)–Cd(1)–O(4)#2	132.67(14)	N(1)–Cd(1)–N(2)	73.2(2)
N(1)–Cd(1)–N(11)#1	96.96(18)	O(4)#2–Cd(1)–N(1)	129.01(19)
N(2)–Cd(1)–N(11)#1	169.6(2)	O(4)#2–Cd(1)–N(2)	96.7(2)
O(4)#2–Cd(1)–N(11)#1	86.73(18)		

Table 1. Selected bond lengths (Å) and angles (deg) for complexes **1** and **2**^a.

^a Symmetry transformations used to generate equivalent atoms: for **1**: #1 $-1/2 + x, -1/2 - y, 1 - z$; #2 $-x, -1/2 + y, 3/2 - z$; for **2**: #1 $1 - x, -1/2 + y, 1/2 - z$; #2 $1 + x, 1/2 - y, 1/2 + z$.

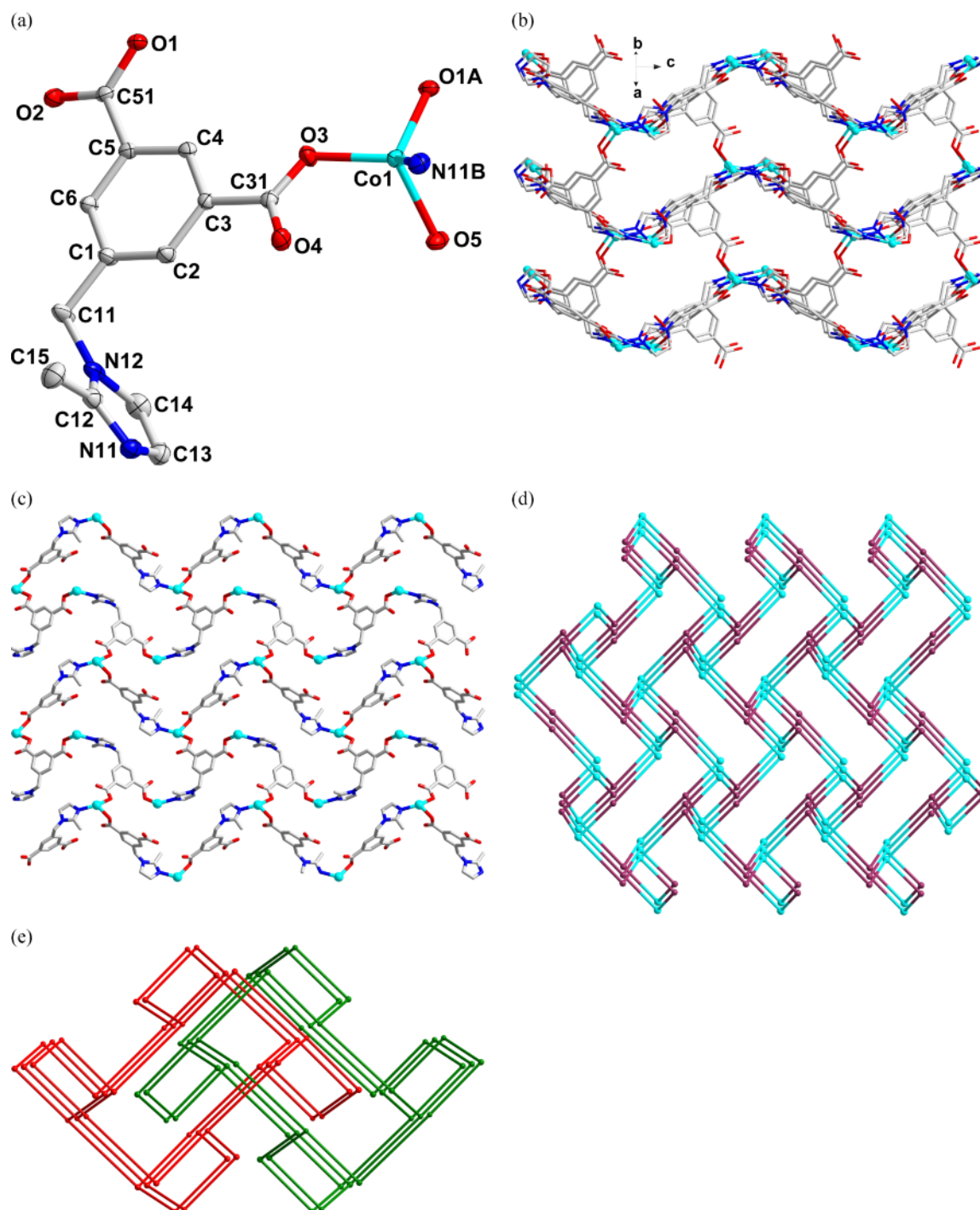


Fig. 1 (color online). (a) The coordination environment of the Co(II) ions in **1** with ellipsoids drawn at the 30% probability level. The hydrogen atoms are omitted for clarity; (b) view of the 3D architecture of **1**. Some organic moieties are omitted for clarity; (c) view of the 2D network in **1**; (d) schematic illustration of the uninodal 3-connected architecture of **1** with (10,3)-a topology; (e) topological representation of 2-fold interpenetrating framework of **1**.

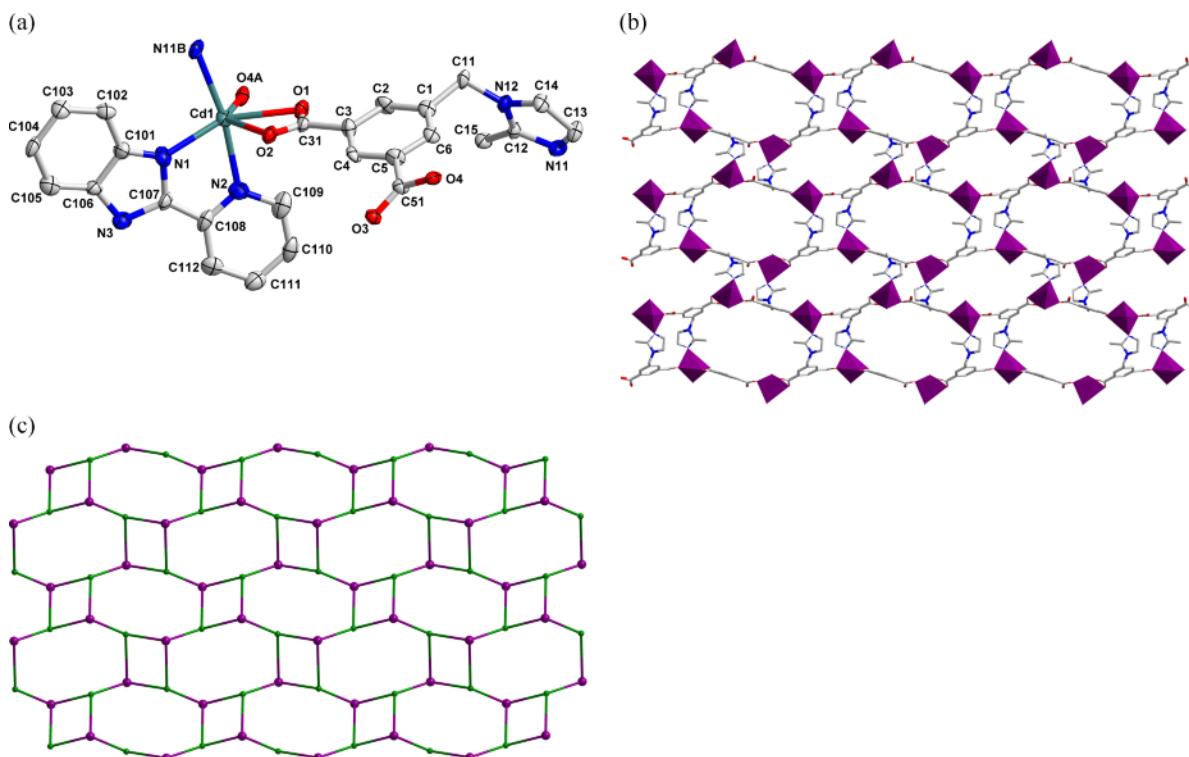


Fig. 2 (color online). (a) The coordination environment of the Cd(II) ions in **2** with ellipsoids drawn at the 30% probability level. The hydrogen atoms are omitted for clarity; (b) view of the 2D network of **2**. Coordinated pybim molecules are omitted for clarity; (c) view of the uninodal 3-connected **fes** network of **2** with $(4,8^2)$ topology.

work structure based on the interconnection of Cd^{2+} cations and the L^{2-} anions. There are one Cd^{2+} cation, one L^{2-} anion, and one pybim molecule in the asymmetrical unit. Each cation is six-coordinated by one methylimidazole and two pybim N atoms and three carboxylate O atoms to furnish a distorted octahedral coordination geometry (Fig. 2a). Three carboxylate O atoms and one pybim N atom define the equatorial plane, and the two apices are occupied by one pybim and one methylimidazole N atom. The bond lengths around the Cd center vary from 2.250(4) to 2.475(4) Å; the bond angles are in the range of 53.94(13) to 169.6(2)°. Two carboxylate groups of the L^{2-} ligand adopt $\mu_1\text{-}\eta^1\text{:}\eta^0$ -monodentate and $\mu_1\text{-}\eta^1\text{:}\eta^1$ -chelating coordination modes, respectively. Each L^{2-} ligand links three Cd^{2+} cations, and each Cd^{2+} cation is surrounded by three L^{2-} ligands. This kind of connection proceeds infinitely to generate a 2D network structure (Fig. 2b). Using topology to analyze the structure, both Cd^{2+} and L^{2-} can be regarded as a 3-connector node,

and thus, the resultant structure of **2** can be simplified as a uninodal 3-connected 2D **fes** network with $(4,8^2)$ topology (Fig. 2c).

PXRD and thermal stability of complexes **1** and **2**

The phase purities of **1** and **2** could be proven by powder X-ray diffraction (PXRD). As shown in Fig. 3, each PXRD pattern of the as-synthesized sample is consistent with the simulated one.

Thermogravimetric analyses (TGA) were carried out for complexes **1** and **2**, and the results are shown in Fig. 4. For complex **1**, weight loss begins at 220 °C corresponding to the release of water, and at 270 °C the rate of weight loss accelerates implying the initiation of decomposition of the framework. At 390 °C the rate of weight loss further speeds up due to accelerated decomposition. For complex **2**, no obvious weight loss can be observed before the decomposition of the framework at 360 °C, which fur-

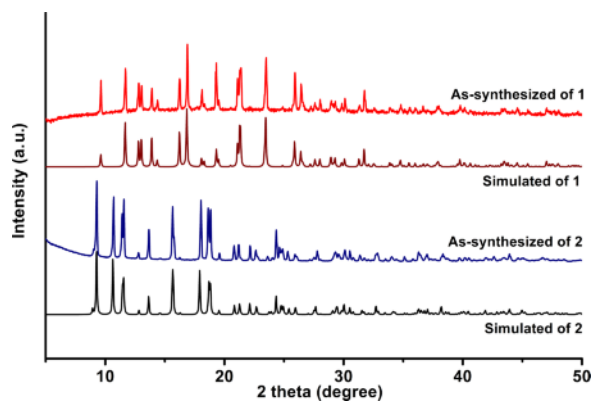


Fig. 3 (color online). The PXRD patterns of complexes **1** and **2**.

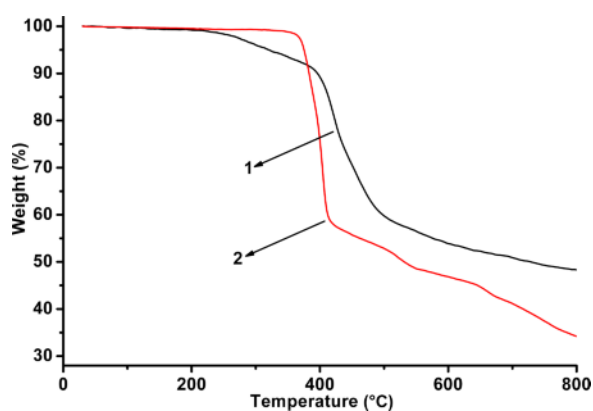


Fig. 4 (color online). TGA curves of complexes **1** and **2**.

ther confirms the absence of solvent in its structure.

Luminescence properties

Previous studies have shown that coordination compounds containing d^{10} metal centers such as Cd(II) may exhibit excellent luminescence properties and have potential applications as photoactive materials [24, 25]. In the present work, the luminescence of complex **2** and the parent H_2L compound has been investigated in the solid state at room temperature. As shown in Fig. 5, intensive emission can be observed with bands at 416 nm ($\lambda_{ex} = 329$ nm) for **2** and 404 nm ($\lambda_{ex} = 348$ nm) for the H_2L ligand. This emission of **2** may be tentatively assigned to intra-ligand transition in the coordinated L^{2-} ligands, since a similar emission

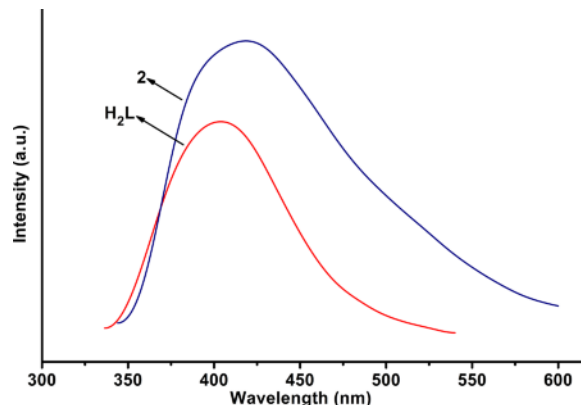


Fig. 5 (color online). Fluorescence of **2** and the H_2L reference in the solid state at room temperature.

was observed for free H_2L [26, 27]. The observation of a blue shift of the emission maximum in complex **2** compared with the free H_2L ligand may originate from the coordination of the ligands to the metal centers [28, 29].

Experimental Section

All commercially available chemicals were of reagent grade and used as received without further purification. The H_2L ligand was synthesized *via* the experimental procedure reported in the literature [29]. Elemental analysis of C, H and N were taken on a Perkin-Elmer 240C elemental analyzer. Infrared spectra (IR) were recorded on a Bruker Vector22 FT-IR spectrophotometer by using KBr pellets. Thermogravimetric analysis (TGA) was performed on a simultaneous SDT 2960 thermal analyzer under nitrogen atmosphere with a heating rate of $10\text{ }^\circ\text{C min}^{-1}$. The luminescence spectra for the powdered solid samples were measured on an Aminco Bowman Series 2 spectrofluorometer with a xenon arc lamp as the light source. In the measurements of emission and excitation spectra the pass width was 5 nm, and all measurements were carried out under the same experimental conditions.

Preparation of $[Co(L)(H_2O)]$ (**1**)

A mixture of $Co(NO_3)_2 \cdot 6H_2O$ (58.2 mg, 0.2 mmol), H_2L (26.0 mg, 0.1 mmol) and KOH (11.2 mg, 0.2 mmol) in 10 mL H_2O was sealed in a 16 mL Teflon-lined stainless-steel container and heated at $180\text{ }^\circ\text{C}$ for 72 h. Then the oven was cooled down at a rate of $10\text{ }^\circ\text{C/h}$. After cooling to room temperature, purple block-shaped crystals of **1** were obtained with an approximate yield of 30% based on H_2L . $C_{13}H_{12}N_2O_5Co$ (335.18): calcd. C 46.58, H 3.61, N 8.36%; found C 46.36, H 3.82, N 8.16%. – IR (KBr pellet, cm^{-1}):

	1	2
Formula	C ₁₃ H ₁₂ N ₂ O ₅ Co	C ₂₅ H ₁₉ N ₅ O ₄ Cd
<i>M_r</i>	335.18	565.85
Crystal size, mm ³	0.20 × 0.20 × 0.20	0.30 × 0.05 × 0.05
Crystal system	orthorhombic	monoclinic
Space group	<i>Pbca</i>	<i>P2₁/c</i>
<i>a</i> , Å	10.5197(7)	12.5340(12)
<i>b</i> , Å	13.5799(9)	15.3220(15)
<i>c</i> , Å	18.3598(12)	15.4480(11)
β, deg	90	127.905(3)
<i>V</i> , Å ³	2622.8(3)	2340.8(4)
<i>Z</i>	8	4
<i>D</i> _{calcd.} , g cm ⁻³	1.70	1.61
μ(MoK _α), cm ⁻¹	1.3	1.0
<i>F</i> (000), e	1368	1136
<i>hkl</i> range	±14, -18 → +13, -20 → +24	±15, -16 → +18, -19 → +18
θ range, deg	2.22–28.36	2.06–26.00
Refl. measured / unique / <i>R</i> _{int}	17861 / 3267 / 0.0271	13835 / 4595 / 0.0133
Param. refined	191	317
<i>R</i> 1(<i>F</i>) / <i>wR</i> 2(<i>F</i> ²) ^{a,b} (all refls.)	0.0424 / 0.0996	0.0656 / 0.1198
GoF (<i>F</i> ²) ^c	1.043	1.022
Δρ _{fin} (max / min), e Å ⁻³	0.88 / -0.36	0.73 / -0.49

Table 2. Crystal structure data for **1** and **2**.

^a $R1 = \sum ||F_o| - |F_c|| / \sum |F_o|$; ^b $wR2 = [\sum w(F_o^2 - F_c^2)^2 / \sum w(F_o^2)^2]^{1/2}$, $w = [\sigma^2(F_o^2) + (AP)^2 + BP]^{-1}$, where $P = (\text{Max}(F_o^2, 0) + 2F_c^2) / 3$; ^c $\text{GoF} = [\sum w(F_o^2 - F_c^2)^2 / (n_{\text{obs}} - n_{\text{param}})]^{1/2}$.

$\nu = 3098$ (m), 1614 (s), 1557 (s), 1512 (m), 1489 (m), 1461 (m), 1422 (s), 1376 (s), 1342 (s), 1280 (m), 1229 (m), 1133 (m), 1099 (m), 1002 (m), 929 (m), 861 (m), 789 (m), 765 (s), 730 (s), 674 (m).

Preparation of [Cd(L)(pybim)] (**2**)

A mixture of Cd(NO₃)₂·4H₂O (61.8 mg, 0.2 mmol), H₂L (26.0 mg, 0.1 mmol), pybim (19.5 mg, 0.1 mmol) and KOH (11.2 mg, 0.2 mmol) in 10 mL H₂O was sealed in a 16 mL Teflon-lined stainless-steel container and heated at 180 °C for 48 h. Then the oven was shut off and cooled down naturally to ambient temperature. After cooling to room temperature, colorless needle-shaped crystals of **2** were obtained with an approximate yield of 25% based on H₂L. C₂₅H₁₉N₅O₄Cd (360.62): calcd. C 53.06, H 3.38, N 12.38%; found C 52.86, H 3.65, N 12.53%. – IR (KBr pellet, cm⁻¹): $\nu = 2975$ (m), 1616 (s), 1565 (s), 1503 (m), 1480 (m), 1452 (s), 1418 (s), 1372 (s), 1321 (s), 1282 (s), 1242 (m), 1152 (m), 1101 (m), 1050 (m), 1004 (m), 976 (m), 897 (m), 812 (m), 749 (s), 727 (s), 698 (m), 676 (m), 636 (m).

Note: excessive metal salts were used in the preparation of **1** and **2** in order to enhance the conversion rate of H₂L.

X-Ray structure determination

Powder X-ray diffraction (PXRD) patterns were measured on a Shimadzu XRD-6000 X-ray diffractometer with CuK_α ($\lambda = 1.5418$ Å) radiation at room temperature.

The crystallographic data collections on single crystals of complexes **1** and **2** were carried out on a Bruker Smart ApexII CCD area-detector diffractometer using graphite-monochromatized MoK_α radiation ($\lambda = 0.71073$ Å) at 293(2) K. The diffraction data were integrated by using the program SAINT [30], which was also used for the intensity corrections for Lorentz and polarization effects. Semi-empirical absorption corrections were applied using the program SADABS [31]. The structures of **1** and **2** were solved by Direct Methods, and all non-hydrogen atoms were refined anisotropically on *F*² by the full-matrix least-squares techniques using the SHELXL-97 crystallographic software package [32–34]. In **1** and **2**, all hydrogen atoms attached to C atoms were generated geometrically; the hydrogen atoms at N and O could be found at reasonable positions in the difference Fourier maps. The crystal parameters and details of the data collections and structure refinements are summarized in Table 2.

CCDC 943613 and 943614 contain the supplementary crystallographic data for this paper. These data can be obtained free of charge from The Cambridge Crystallographic Data Centre via www.ccdc.cam.ac.uk/data_request/cif.

Acknowledgement

The authors gratefully acknowledge the special fund for promotion programs of industry-university-research cooperation of Huaian Administration of Science & Technology (HC201216) for financial support of this work.

- [1] Y. Kobayashi, B. Jacobs, M. D. Allendorf, J. R. Long, *Chem. Mater.* **2010**, *22*, 4120–4122.
- [2] T. Uemura, Y. Ono, Y. Hijikata, S. Kitagawa, *J. Am. Chem. Soc.* **2010**, *132*, 4917–4924.
- [3] L. F. Ma, X. Q. Li, L. Y. Wang, H. W. Hou, *CrystEngComm* **2011**, *13*, 4625–4634.
- [4] B. H. Ye, M. L. Tong, X. M. Chen, *Coord. Chem. Rev.* **2005**, *249*, 545–565.
- [5] J. R. Li, R. J. Kuppler, H. C. Zhou, *Chem. Soc. Rev.* **2009**, *38*, 1477–1504.
- [6] S. Hasegawa, S. Horike, R. Matsuda, S. Furukawa, K. Mochizuki, Y. Kinoshita, S. Kitagawa, *J. Am. Chem. Soc.* **2007**, *129*, 2607–2614.
- [7] H. W. Kuai, X. C. Cheng, X. H. Zhu, *Z. Naturforsch.* **2013**, *68b*, 147–154.
- [8] X. C. Cheng, H. W. Kuai, *Z. Naturforsch.* **2012**, *67b*, 1255–1262.
- [9] X. C. Cheng, X. H. Zhu, H. W. Kuai, *Z. Naturforsch.* **2012**, *67b*, 1248–1254.
- [10] K. L. Zhang, Y. Chang, C. T. Hou, G. W. Diao, R. T. Wu, S. W. Ng, *CrystEngComm* **2010**, *12*, 1194–1204.
- [11] H. W. Kuai, X. C. Cheng, X. H. Zhu, *Polyhedron* **2013**, *50*, 390–397.
- [12] H. W. Kuai, X. C. Cheng, X. H. Zhu, *Polyhedron* **2013**, *53*, 113–121.
- [13] S. S. Chen, M. Chen, S. Takamizawa, M. S. Chen, Z. Su, W. Y. Sun, *Chem. Commun.* **2011**, *47*, 752–754.
- [14] S. S. Chen, M. Chen, S. Takamizawa, P. Wang, G. C. Lv, W. Y. Sun, *Chem. Commun.* **2011**, *47*, 4902–4904.
- [15] Z. Su, M. Chen, T. Okamura, M. S. Chen, S. S. Chen, W. Y. Sun, *Inorg. Chem.* **2011**, *50*, 985–991.
- [16] R. Patra, I. Goldberg, *Acta Crystallogr.* **2013**, *C69*, 344–347.
- [17] H. W. Kuai, X. C. Cheng, X. H. Zhu, *Inorg. Chem. Commun.* **2012**, *25*, 43–47.
- [18] H. W. Kuai, X. C. Cheng, X. H. Zhu, *J. Coord. Chem.* **2011**, *64*, 3323–3332.
- [19] H. W. Kuai, X. C. Cheng, L. D. Feng, X. H. Zhu, *Z. Anorg. Allg. Chem.* **2011**, *637*, 1560–1565.
- [20] H. W. Kuai, X. C. Cheng, X. H. Zhu, *J. Coord. Chem.* **2011**, *64*, 1636–1644.
- [21] H. W. Kuai, T. A. Okamura, W. Y. Sun, *J. Coord. Chem.* **2012**, *65*, 3147–3159.
- [22] H. W. Kuai, C. Hou, W. Y. Sun, *Polyhedron* **2013**, *52*, 1268–1275.
- [23] V. A. Blatov, *IUCr CompComm Newsletter* **2006**, *7*, 4–38.
- [24] Y. B. Dong, P. Wang, R. Q. Huang, M. D. Smith, *Inorg. Chem.* **2004**, *43*, 4727–4739.
- [25] D. M. Ciurtin, N. G. Pschirer, M. D. Smith, U. H. F. Bunz, H. C. zur Loye, *Chem. Mater.* **2001**, *13*, 2743–2745.
- [26] H. W. Kuai, X. C. Cheng, X. H. Zhu, *J. Coord. Chem.* **2013**, *66*, 28–41.
- [27] B. Valeur, *Molecular Fluorescence: Principles and Applications*, Wiley-VCH, Weinheim, **2002**.
- [28] Y. Q. Huang, B. Ding, H. B. Song, B. Zhao, P. Ren, P. Cheng, H. G. Wang, D. Z. Liao, S. P. Yan, *Chem. Commun.* **2006**, 4906–4908.
- [29] H. W. Kuai, J. Fan, Q. Liu, W. Y. Sun, *CrystEngComm* **2012**, *14*, 3708–3716.
- [30] SAINT, Program for Data Extraction and Reduction, Bruker Analytical X-ray Instruments Inc., Madison, Wisconsin (USA) **2001**.
- [31] G. M. Sheldrick, SADABS, Program for Area Detector Absorption Correction, University of Göttingen, Göttingen (Germany) **1997**.
- [32] G. M. Sheldrick, SHELXS/L-97, Programs for Crystal Structure Determination, University of Göttingen, Göttingen (Germany) **1997**.
- [33] G. M. Sheldrick, *Acta Crystallogr.* **1990**, *A46*, 467–473.
- [34] G. M. Sheldrick, *Acta Crystallogr.* **2008**, *A64*, 112–122.